Pilot Pattern Optimization for Small Data Packet Transmission

Ljiljana Marijanović, *Student Member, IEEE*, Stefan Schwarz, *Member, IEEE*, and
Markus Rupp, *Senior Member, IEEE*

Abstract—We consider pilot pattern optimization for single user single-input-single-output orthogonal frequency division multiplexing transmission over doubly-selective channels, assuming least squares channel estimation with linear interpolation and extrapolation. Our focus is on small data packet transmission which is typical for machine-type communications. We compare diamond-shaped pilot patterns to rectangular-shaped pilot patterns. We optimize the density and spacing of pilot symbols in both pilot patterns with respect to the constrained capacity and demonstrate that the rectangular pilot pattern can outperform the diamond-shaped pattern in case of small data packet transmission.

Index Terms—Border Effects, Channel Estimation Error, Constrained Capacity, Extrapolation Error, Pilot Pattern Optimization

I. Introduction

One of the major design goals of the upcoming fifth generation (5G) of wireless communications technology is to support highly efficient transmission of small data packets [1]. Ultra-reliable low latency communications (URLLC), as one of the 5G use cases, requires short data packets in order to minimize latency [1], [2], [3], [4].

In this paper we consider Single User Single-Input-Single-Output (SU-SISO) Orthogonal Frequency Division Multiplexing (OFDM) for small data packet transmission. In order to evaluate the capacity performance assuming doubly-selective channels we account not only for different channel conditions such as delay and Doppler spread, but also for the channel estimation error as a consequence of imperfect channel knowledge [5]. Moreover, we investigate the optimal pilot pattern in order to maximize the constrained capacity for a given total number of pilots. For our optimization problem we rely on the cost function investigated in [6].

In the literature a diamond pilot pattern or its variants, such as rotated diamond or cell pattern are presented as optimal, mainly due to the unbounded transmission bandwidth [7]. However, in reality with finite bandwidth the optimal pilot pattern also depends on the extrapolation error that is involved in the channel estimation error. The extrapolation error depends on the number of data resources placed out of the certain pilot shape. In general, placing the pilots closer

Marijanović, Ljiljana, Institute of Telecommunications, Technische Universität (TU) Wien, Gusshausstrasse 25/389, 1040 Vienna, Austria (e-mail: ljiljana.marijanovic@nt.tuwien.ac.at)

Schwarz, Stefan, Institute of Telecommunications, Technische Universität (TU) Wien, Gusshausstrasse 25/389, 1040 Vienna, Austria (e-mail: sschwarz@nt.tuwien.ac.at)

Rupp, Markus, Institute of Telecommunications, Technische Universität (TU) Wien, Gusshausstrasse 25/389, 1040 Vienna, Austria (e-mail: mrupp@nt.tuwien.ac.at)

Marijanović, Lj. and Schwarz, S. are with Christian Doppler Laboratory for Dependable Wireless Connectivity for the Society in Motion.

to the border results in a smaller extrapolation error. In case of large transmit bandwidth, the impact of the extrapolation error is negligible; however, for small transmit bandwidth this is not the case.

Assuming a small bandwidth we compare rectangular pilot patterns and diamond pilot patterns and emphasize the superiority of rectangular pilot patterns in certain cases due to the smaller extrapolation error.

The rest of this work is structured as follows: Section II provides an overview of the system model. In Section III we provide the criterion for the pilot pattern optimization. The simulation results and comparison between different pilot patterns are shown in Section IV.

II. System Model

As mentioned before, we consider SU-SISO OFDM. The received OFDM symbol is represented as:

$$y_{k,n} = h_{k,n} x_{k,n} + \omega_{k,n} \qquad (1)$$

where $h_{k,n} \in \mathbb{C}$ denotes the frequency response and $x_{k,n} \in \mathbb{C}$ denotes the transmitted data symbol at appropriate frequency-time position k, n. Additive white Gaussian noise and intercarrier interference (ICI) are included in $\omega_{k,n} \sim \mathcal{CN}(0, \sigma_{ICI}^2 + \sigma_n^2)$, with σ_n^2 denoting the noise power and σ_{ICI}^2 denoting the average ICI power as a consequence of Doppler shifts. In order to estimate the channel on pilot positions, we perform Least Squares (LS) estimation:

$$\hat{h}_{k_p,n_p} = \frac{y_{k_p,n_p}}{x_{k_p,n_p}}, \qquad (2)$$

where $k_p, n_p \in \mathcal{P}$ denotes a pilot position from the set $\mathcal{P}$ of all pilot positions. The estimated channel at the pilot positions enables to find the channel estimates at data positions $\hat{h}_{k,n}$, by applying a two dimensional (2D) linear interpolation:

$$\hat{h}_{k,n} = \sum_{k_p,n_p \in \mathcal{P}} w_{k,n}^{\{k_p,n_p\}} \hat{h}_{k_p,n_p}. \qquad (3)$$

Here, $w_{k,n}^{\{k_p,n_p\}}$ denotes the inter/extrapolation weight of the estimated channel at pilot position k_p, n_p with respect to the inter/extrapolated data position k, n.

III. Pilot Pattern Optimization

As mentioned above, we compare diamond-shaped pilot patterns and rectangular-shaped pilot patterns in this work. In contrast to the common assumption of equally spaced pilots in the time and frequency domains, which is a reasonable assumption for unbounded transmission bandwidth and duration, we consider unequally spaced pilots, which allows us to achieve a smaller extrapolation error.
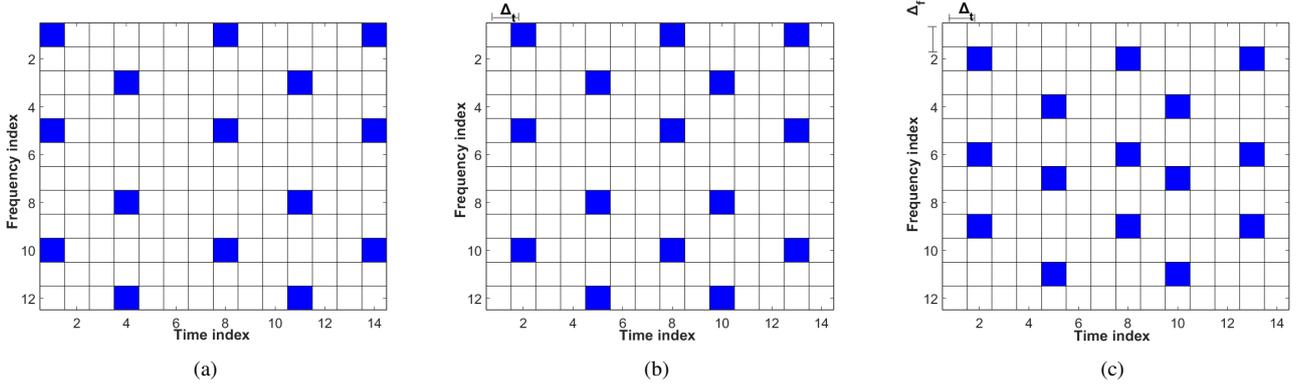
Fig. 1: Pilot shifts in time and frequency domain for a constant bandwidth

To optimize the spacing of pilot symbols, we employ the constrained capacity as a cost function [8]:

$$\bar{C}(N_f, N_t, \Delta_f, \Delta_t) = B(N_f, N_t) \log_2(1 + \bar{\gamma}(N_f, N_t, \Delta_f, \Delta_t)). \tag{4}$$

In this equation $B(N_f, N_t)$ refers to the spectral utilization function depending on the number of pilots in time N_t, and frequency N_f, respectively. It is defined as:

$$B(N_f, N_t) = \frac{N_d}{N_d + N_p}, \tag{5}$$

where N_d and $N_p = N_t N_f$ are the number of transmitted data and the number of pilots, respectively. The optimal pilot density depends on the channel properties. For example, with large delay and Doppler spread the pilot density will be increased in frequency and time domain, respectively. It further affects the number of data and pilots within the corresponding bandwidth. The post-equalization Signal to Interference Plus Noise Ratio (SINR) is denoted by $\bar{\gamma}$ and it is stated as:

$$\bar{\gamma}(N_f, N_t, \Delta_f, \Delta_t) = \frac{\sigma_d^2}{\sigma_n^2 + \sigma_{ICI}^2 \sigma_d^2 + \sigma_e^2(N_f, N_t, \Delta_f, \Delta_t) \sigma_d^2}, \tag{6}$$

where σ_d^2 is the unit data power and σ_e^2 is the channel estimation error. Modeling the channel according to the Jakes' spectrum, ICI is represented by the zeroth-order Bessel function of the first kind [9]. The ICI power also impacts the channel estimation error. The closed-form expression of the channel estimation error is given by:

$$\sigma_e^2(N_f, N_t, \Delta_f, \Delta_t) = c_e(N_f, N_t, \Delta_f, \Delta_t)(\sigma_n^2 + \sigma_{ICI}^2 \sigma_d^2)$$
$$+ d(N_f, N_t, \Delta_f, \Delta_t), \tag{7}$$

with d denoting the interpolation error and c_e denoting the coefficient determined by the weighting factor from (3):

$$c_e(N_f, N_t, \Delta_f, \Delta_t) = \frac{1}{N_d} \sum_{\{k,n\} \in \mathfrak{D}} \sum_{\{k_p, n_p\} \in \mathcal{P}} \left(w_{k,n}^{\{k_p, n_p\}} \right)^2. \tag{8}$$

The scalar c_e is the averaged value over all data symbols from the data set $\mathfrak{D}$, depending only on the pilot positions. Taking into account not only the pilot positions, but also the second-order statistics captured by the autocorrelation function $R_{(\Delta k, \Delta n)}$, the interpolation error can be expressed by:

$$d = \frac{1}{N_d} \sum_{\{k,n\} \in \mathfrak{D}} \left(1 - 2 \sum_{\{k_p, n_p\} \in \mathcal{P}} w_{k,n}^{\{k_p, n_p\}} \Re\{R_{(\Delta k, \Delta n)}\} \right.$$
$$\left. + \sum_{\{k_p, n_p\} \in \mathcal{P}} \sum_{\{k_{p'}, n_{p'}\} \in \mathcal{P}} w_{k,n}^{\{k_p, n_p\}} w_{k,n}^{\{k_{p'}, n_{p'}\}} \Re\{R_{(\Delta k_{pp'}, \Delta n_{pp'})}\} \right). \tag{9}$$

Due to space issues we omit the dependence of d on the variables N_f, N_t, Δ_f and Δ_t. Under the Wide Sense Stationary Uncorrelated Scattering (WSSUS) assumption, the autocorrelation function is defined as a product of temporal and frequency correlation:

$$R_{(\Delta k, \Delta n)} = R_{\Delta k} R_{\Delta n}. \tag{10}$$

Since we assume Jakes' spectrum the temporal correlation is given by the zeroth-order Bessel function of the first kind. Frequency correlation is calculated according to the power delay profile of the channel. In order to have smaller extra/interpolation error both time and frequency correlation have to be strong. As we emphasized before, we do not only observe the pilot spacings in time and frequency domain, but also the pilot placement relevant to the proximity of the border of the transmit block in order to evaluate the extrapolation error. In other words, we artificially place the pilots at the border of our transmit block and shift them symmetrically keeping the bandwidth constant. We shift the pilots either particularly in time, Δ_t or frequency domain, Δ_f or in both domains simultaneously, as it is shown in Figure 1. Figure 1a represents the case when pilots are placed at the border of the transmit block, while Figures 1b and 1c are cases with only time shift and shifts in both domains, respectively. This case shows the diamond pilot pattern. The same setup holds for the rectangular pilot pattern. The optimal time-frequency shifts change depending on the channel conditions and bandwidth size.

IV. SIMULATION RESULTS

In this section, we compare the performance of the constrained capacity of the diamond pilot pattern and the rectangular pilot pattern as a function of the user velocity and the number of pilots in time and frequency domain. We consider a doubly-selective channel and optimize the constrained capacity with respect to the pilot symbol spacing for a given total number of pilot symbols. Additionally, we simulate the throughput performance according to the

optimal pilot density in order to verify the validity of our analytical results. The parameters we use for the analysis as well as for simulations are shown in Table 1.

TABLE 1: Parameters used for the results.

Parameters	Values
Number of Subcarriers	12, 72
Subcarrier Spacing	15kHz
Channel Model	Pedestrian A, Vehicular A
SNR	15dB
Delay spread	45ns - PedA, 370ns - VehA
Modulation coding scheme	Adaptive

Our goal is to maximize the constrained capacity and find the optimal number of pilots in frequency and time domain, according to the channel. In Figure 2 we show the behavior of the constrained capacity versus the number of pilots in frequency domain when the SNR is 15 dB. We consider two different velocities of 5 km/h for the Pedestrian A channel and 150 km/h for the Vehicular A channel [10]. We take the optimal frequency and time distance between the pilots and optimal time-frequency shifts at the same time. In both cases we can observe that the rectangular pilot pattern outperforms the diamond pilot pattern due to the smaller extrapolation error. Similarly, in Figure 3 we present how the constrained capacity changes with respect to different N_t. Here, we can see that the rectangular pilot pattern is better when we have sufficiently flat channel. However, in selective channels that is the case only when the number of pilots in time domain is small, emphasizing the impact of the extrapolation error due to the larger border effects. Once the number of pilots is sufficient to mitigate the border effect, the diamond pilot pattern achieves better rate. Figure 4 shows how the constrained capacity changes with respect to different velocities for the optimal configuration of parameters. If the noise power is sufficiently large, then the channel estimation error is mainly determined by the extrapolation error (7), resulting in better behavior of the rectangular pilot pattern. On the other hand, if the noise power is small, then the interpolation error determines the channel estimation error and in such cases the diamond pilot pattern overcomes the rectangular pilot pattern.

In order to verify the validity of the SINR closed-form expression (6) accounting also for the extrapolation error we simulate the throughput performance employing the *5G Link Level Simulator* [11]. Here, we use a larger packet size of 72 subcarriers for analysis as well as for simulations. For certain number of pilots in the frequency and the time domain we find the optimal throughput, using adaptive modulation and coding schemes. From Figure 5 it is visible that our simulated throughput performance has the same trend as the constrained capacity. There is a small mismatching between the analytical and simulation result due to the channel estimation error. That is a consequence of an assumption of equally distributed power over infinite number of subcarriers for ICI power calculation. However, we assume a small bandwidth in the simulations where subcarriers at the edge of the transmission bandwidth do not experience the same transmit power as subcarriers in the middle. We can observe that the behavior is almost constant over a large regime of pilots in time and frequency.
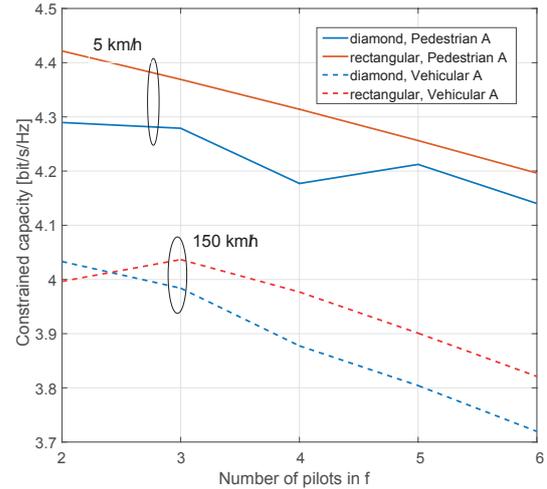

Fig. 2: Constrained capacity vs. number of pilots in frequency
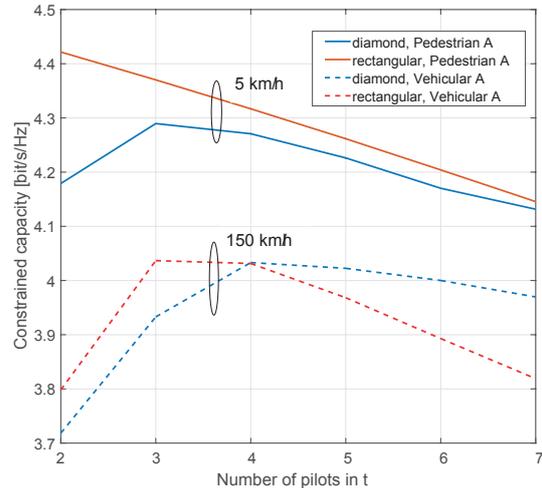

Fig. 3: Constrained capacity vs. number of pilots in time
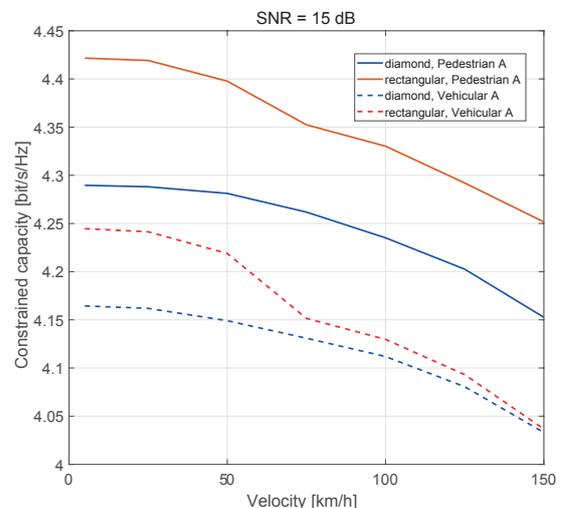

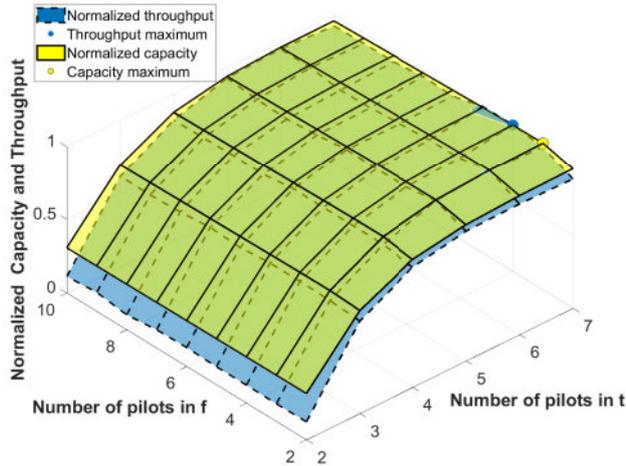Fig. 4: Constrained capacity vs. velocity

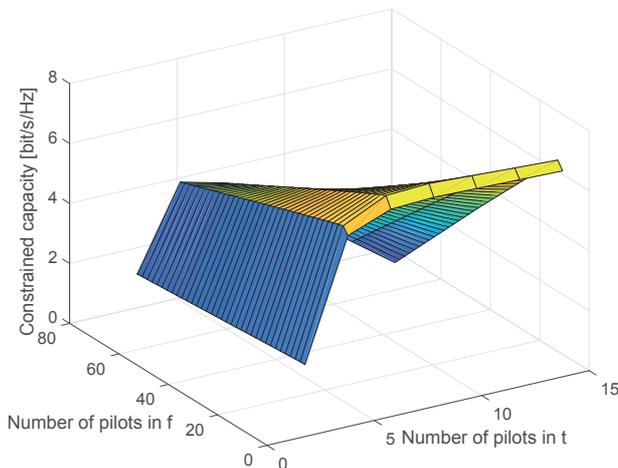Fig. 5: Comparison of normalized capacity and normalized throughput

Fig. 6: Constrained capacity as a function of the number of pilots

In this area a larger overhead is compensated by an SINR gain or more precisely by the small interpolation error due to the large number of pilots. However, once the overhead gets too large the constrained capacity performance starts deteriorating. In that scenario the impact of the bandwidth is much larger than the impact of inter/extrapolation error, Figure 6.

V. CONCLUSION

In this paper, we compare the performance of diamond-shaped and rectangular pilot patterns for small transmission bandwidth assuming LS channel estimation with linear interpolation and extrapolation. We show that the rectangular pattern can outperform the diamond-shaped pattern in case of strongly emphasized border effects. This is a consequence of reduced extrapolation error of the rectangular pattern at the border of the transmission bandwidth. Contrarily, the diamond shaped pattern achieves a lower interpolation error in strongly time-selective situations, which can compensate for the larger extrapolation error. In this

situation the diamond pattern outperforms the rectangular pattern. Additionally, we compare the simulated throughput performance to the analytical constrained capacity in order to confirm the validity of the SINR closed-form expression. We observe that the performance of both functions match quite well with small deviations, mainly due to the assumption of the small bandwidth.

REFERENCES

[1] S. Schwarz and M. Rupp, "Society in motion: Challenges for LTE and beyond mobile communications," *IEEE Communications Magazine*, vol. 54, no. 5, pp. 76–83, 2016.

[2] G. Durisi, T. Koch, and P. Popovski, "Toward massive, ultrareliable, and low-latency wireless communication with short packets," *Proceedings of the IEEE*, vol. 104, no. 9, pp. 1711–1726, 2016.

[3] B. Lee, S. Park, D. J. Love, H. Ji, and B. Shim, "Packet structure and receiver design for low-latency communications with ultra-small packets," in *Global Communications Conference (GLOBECOM), 2016 IEEE*. IEEE, 2016, pp. 1–6.

[4] L. Marijanović, S. Schwarz, and M. Rupp, "Intercarrier interference of multiple access UFMC with flexible subcarrier spacings," in *25th European Signal Processing Conference (EUSIPCO), 2017*. IEEE, 2017, pp. 888–892.

[5] M. Liu, M. Crussiere, and J.-F. Hélard, "Enhanced two-dimensional data-aided channel estimation for TDS-OFDM," in *4th International Conference on Signal Processing and Communication Systems (ICSPCS), 2010*. IEEE, 2010, pp. 1–7.

[6] M. Šimko, Q. Wang, and M. Rupp, "Optimal pilot pattern for time variant channels," in *(ICC), 2013 IEEE International Conference on Communications*. IEEE, 2013, pp. 5420–5424.

[7] J.-W. Choi and Y.-H. Lee, "Optimum pilot pattern for channel estimation in OFDM systems," *IEEE Transactions on Wireless Communications*, vol. 4, no. 5, pp. 2083–2088, 2005.

[8] M. Šimko, P. S. Diniz, Q. Wang, and M. Rupp, "Adaptive pilot-symbol patterns for MIMO OFDM systems," *IEEE Transactions on Wireless Communications*, vol. 12, no. 9, pp. 4705–4715, 2013.

[9] Y. Li and L. J. Cimini, "Bounds on the interchannel interference of OFDM in time-varying impairments," *IEEE Transactions on Communications*, vol. 49, no. 3, pp. 401–404, 2001.

[10] ITU, "Recommendation ITU-R M.1225: Guidelines for Evaluation of Radio Transmission Technologies for IMT-2000," *International Telecommunication Union, , Tech. Rep*, 1997.

[11] S. Pratschner, B. Tahir, L. Marijanovic, M. Mussbah, K. Kirev, R. Nissel, S. Schwarz, and M. Rupp, "Versatile mobile communications simulation: The Vienna 5G link level simulator," *EURASIP Journal on Wireless Communications and Networking*, 2018.